

# Real-time nanometer-vibration measurement with a self-mixing microchip solid-state laser

Kenju Otsuka, Kazutaka Abe, and Jing-Yuan Ko

*Department of Human and Information Science, Tokai University, 1117 Kitakaname, Hiratsuka, Kanagawa 259-1292, Japan*

Tsong-Shin Lim

*Department of Physics, National Cheng Kung University, Tainan 70101, Taiwan*

Received March 29, 2002

Nanometer vibration analysis of a target has been demonstrated by a self-aligned optical feedback vibrometry technique that uses a laser-diode-pumped microchip solid-state laser. The laser output waveform, which was modulated through interference between a lasing field and an extremely weak ( $< -100$ -dB) frequency-modulated (FM) feedback field, was analyzed by the Hilbert transformation to yield the vibration waveform of the target. Experimental signal characteristics have been reproduced by numerical simulations. Real-time vibration measurement has also been achieved with a simple FM demodulation circuit. © 2002 Optical Society of America

OCIS codes: 120.7280, 140.3480, 140.3580.

Laser-diode-pumped microchip solid-state lasers (DPSSLs) have great technological importance for a wide variety of applications as compact, durable, coherent light sources. The ultrahigh-sensitivity response of DPSSLs to external optical feedback light because of their extremely short photon lifetimes compared with the population lifetimes that are inherent in microchip lasers<sup>1</sup> has resulted in such significant applications as self-aligned laser Doppler velocimetry,<sup>2-4</sup> vibrometry,<sup>5</sup> and imaging.<sup>5,6</sup> In conventional sensing techniques, sophisticated interferometric optics and highly sensitive electronics are required for detection of the photomixing signal between a lasing field and an extremely weak, scattered field from the object.<sup>7-9</sup> In contrast, the present technique utilizes a highly sensitive self-mixing modulation effect<sup>1,2,10-13</sup> in microchip solid-state lasers without using highly sensitive electronics and makes the laser act as a high-efficiency mixer-oscillator and a shot-noise-limited quantum detector. In DPSSLs the effective long-term interference between a lasing field and a coherent component of a scattered field that is fed back to the microcavity laser resonator occurs because of the high degree of coherence of the lasing field. In this Letter we demonstrate real-time nanometer-vibration measurements by using a DPSSL and this self-mixing modulation technique.

The experimental setup is shown in Fig. 1. A 7-mm  $\times$  7-mm *c* plate Nd direct compound LiNdP<sub>4</sub>O<sub>12</sub> (LNP) laser with a 1-mm-thick plane-parallel Fabry-Perot cavity was used. An end surface was coated to be transmissive at the laser-diode pump wavelength of 808 nm (85% transmission) and highly reflective (99.9%) at the lasing wavelength,  $\lambda = 1320$  nm. The other surface was coated to be 1% transmissive at the lasing wavelength. The collimated laser-diode pump light was passed through anamorphic prism pairs, which transformed the elliptical beam into a circular beam, and was focused onto the LNP crystal by a microscope objective lens of 20 $\times$  magnification. A part (96%) of the output light was frequency shifted by two acousto-optic modulators (AOMs) and

impinged upon a speaker that had an Al-coated surface with an average roughness of 100  $\mu$ m that was placed 90 cm from the laser. Because the central frequency of AOMs was 80 MHz, we used two AOMs to achieve appropriate frequency shifts of the order of 1 MHz for experiments. By changing the modulation frequencies of upshifted and downshifted AOMs (PbMoO<sub>4</sub>; Hoya-Schott Model A-150, 80-MHz central frequency) we shifted the optical carrier frequency by 500 kHz–5 MHz after a round trip for the feedback field. Another part (4%) of the output light was detected by an InGaAs photoreceiver (New Focus Model 1811, dc, 125 MHz). Depending on the measurement procedures, we used a frequency demodulation circuit, a digital oscilloscope (Tektronix Model TDS 540D, dc, 500 MHz) connected to a personal computer, and a rf spectrum analyzer (Tektronix 3026, dc, 3 GHz).

First let us briefly describe the results of long-term averaged measurements of the vibrating target. Figure 2(a) shows power spectra (long-time average) for several voltages applied to the speaker when the average was 4000 and the resolution of the spectrum analyzer was 300 Hz. The LNP laser output power was 5 mW, and the power of the light that impinged upon the InGaAs detector was 200  $\mu$ W. From the intensity ratios of the carrier and sideband

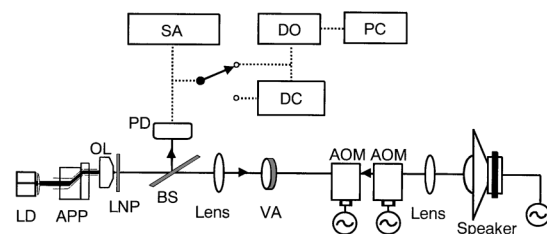


Fig. 1. Experimental configuration of self-mixing laser-Doppler vibrometry and optical microphony: LD, laser diode; APP, anamorphic prism pairs; OL, microscope objective lens; BS, glass-plate beam splitter; PD, photodiode receiver; SA, rf spectrum analyzer; VA, variable attenuator; DO, digital oscilloscope; DC, frequency demodulation circuit; PC, personal computer.

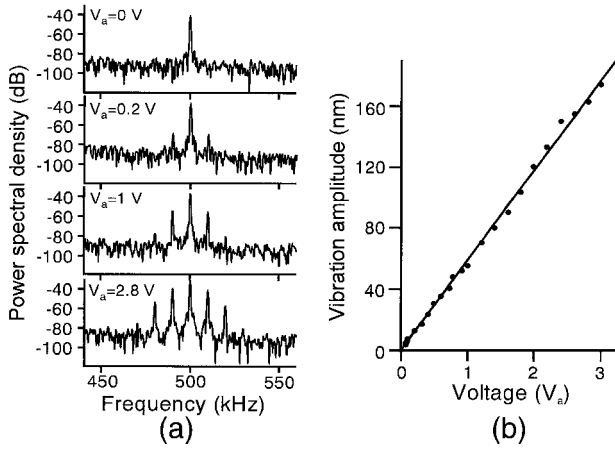


Fig. 2. (a) Power spectra (long-time average) for several applied voltages. (b) Maximum vibration amplitude versus voltage applied to the speaker. The LNP output power was 5 mW. Carrier frequency,  $\Delta\omega/2\pi = 500$  kHz; modulation frequency,  $f_m = \omega_m/2\pi = 8.42$  kHz.

components, i.e., frequency modulation index  $\beta$ , we estimated the maximum vibration amplitude  $A_{v,m}$  by using the relationship  $A_{v,m} = \lambda\beta/2\pi$ . The measured vibration amplitudes at the modulation frequency of 8.42 kHz with the carrier frequency of 500 kHz are plotted in Fig. 2(b) as a function of applied voltage  $V_a$  and yielded the relation  $A_{v,m}/V_a = 59$  [nm/V] for the speaker that we used. The carrier-to-noise ratio in the absence of voltage to the speaker was 55 dB, yielding a measurable minimum vibration amplitude of 1 nm. The velocity range that we were able to measure in the present self-mixing vibrometry with the speaker was 1  $\mu\text{m/s}$ –10 cm/s in the vibration frequency range 20 Hz–20 kHz. Measurable maximum velocity in the self-mixing velocimetry scheme reached 10 m/s.<sup>3</sup> This result implies that the present vibrometry system can apply to ultrasonic vibration measurement up to 1 MHz.

Next, to measure temporal evolutions of nanometer vibrations  $A_v(t)$  we analyzed modulated output waveforms by using the Hilbert transformation. From this transformation of time series, i.e., Gabor's analytic signal,<sup>14</sup> we calculated the analytic phase of the modulated signal by using LabView software on a PC and deduced vibration amplitude  $A_v(t)$  from phase difference  $\Delta\Phi(t)$  between the reference (carrier) signal and the modulated signal by using the relation  $A_v(t) = \lambda\Delta\Phi(t)$ . Analytic phase  $\Phi_A$  is related to analytic signal  $V_A$  and its time average  $\langle V_A \rangle$  by  $V_A(t) - \langle V_A \rangle = R_A(t)\exp[i\Phi_A(t)]$ . Here,  $V_A(t) = I(t) + iI_H(t)$ , where  $I(t)$  is the time series of the scalar intensity and  $I_H$  is its Hilbert transform. Figure 3 shows modulated output waveforms and corresponding vibration waveforms for different feedback ratios, where we used a variable optical attenuator to change the feedback ratio. Although the modulated output intensity decreased with a decreasing feedback ratio, vibration waveforms were found to be reproduced well.

It was impossible to measure the feedback ratio of a scattered field from the speaker into the laser experimentally. Therefore, to reproduce the experimental

signal characteristics and estimate the feedback ratio accurately from the correspondence between experimental and numerical results, we carried out numerical simulations of the following model equations, that is, lasers with frequency-modulated optical feedback<sup>5,15,16</sup>:

$$dN(t)/dt = K\{w - 1 - N(t) - [1 + 2N(t)]E(t)^2\}, \quad (1)$$

$$dE(t)/dt = N(t)E(t) + mE(t - t_D) \times \cos \Psi(t) + \{2\epsilon[N(t) + 1]\}^{1/2}\xi(t), \quad (2)$$

$$d\phi(t)/dt = [E(t - t_D)/E(t)]\sin \Psi(t), \quad (3)$$

$$\Psi(t) = \Delta\Omega t + \beta \sin \Omega_m t - \phi(t) + \phi(t - t_D) - (\Omega_0 + \Delta\Omega/2)t_D. \quad (4)$$

Here,  $E(t)$  is the normalized field amplitude,  $N(t)$  is the normalized excess population inversion,  $w = P/P_{\text{th}}$  is the relative pump power normalized by the threshold,  $K = \tau/\tau_p$  is the population-to-photon lifetime ratio,  $\phi(t)$  is the phase of the lasing field,  $\Psi(t)$  is the phase difference between the lasing and the feedback fields,  $\Delta\Omega = \omega_i\tau_p - \omega_0\tau_p$  is the normalized frequency shift ( $\tau_p$  is the photon lifetime),  $m$  is the amplitude feedback coefficient,  $\Omega_m = \omega_m\tau_p$  is the normalized modulation frequency, and  $t$  and  $t_D$  are the time and the delay time normalized by the photon lifetime. The last term of Eq. (2) expresses the quantum (spontaneous emission) noise, where  $\epsilon$  is the spontaneous emission rate and  $\xi(t)$  is the Gaussian white noise with zero mean and the value  $\langle \xi(t)\xi(t') \rangle = \delta(t - t')$  that is  $\delta$  correlated in time. The numerical results are shown in Fig. 4, that assuming  $m = 10^{-5}$ . Here the lifetime ratio  $K = 2 \times 10^5$  (i.e.,  $\tau_p = 600$  ps) was determined from the measured dependence of relaxation oscillation frequency  $f_R$  on excess pump, i.e.,  $f_R = (1/2\pi)[(w - 1)/\tau\tau_p]^{1/2}$ , assuming that  $\tau = 120$   $\mu\text{s}$ . We adopted other parameters that correspond to the experiment, i.e., relative pump

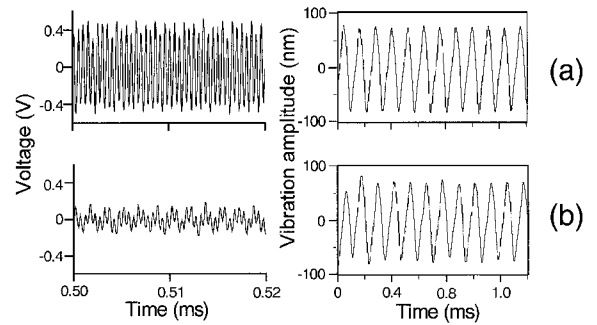


Fig. 3. Left, frequency-modulation waveforms and right, vibration waveforms for different feedback ratios (a) without an attenuator, in which the nominal feedback ratio is estimated to be  $-100$  dB from correspondence with the numerical result, and (b) for an additional attenuation value of  $-12.0$  dB. Carrier frequency, 2 MHz; modulation frequency, 8.42 kHz; applied voltage, 1 V.

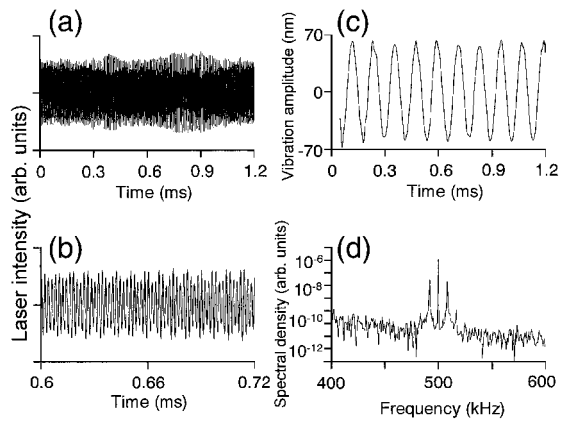


Fig. 4. Numerical results: (a) modulated waveform, (b) detailed waveform, (c) vibration amplitude, (d) power spectrum (long-time average).

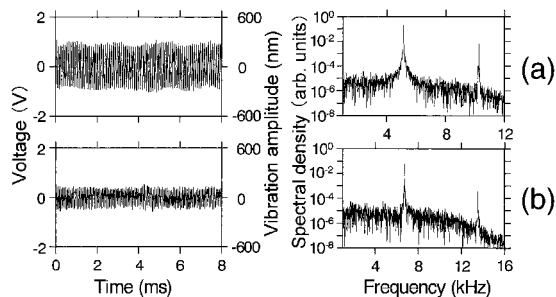


Fig. 5. *In situ* measurement of vibration waveforms and their power spectra for different modulation frequencies. Modulation frequency  $f_m$ : (a) 5.13 kHz, (b) 6.75 kHz. Applied voltage, 1 V; carrier frequency, 2 MHz.

power  $w = 1.2$  (i.e., pump power  $P = 200$  mW); round-trip frequency shift (i.e., carrier frequency)  $\Delta f = 500$  kHz; modulation frequency  $f_m = 8.42$  kHz;  $\beta = 0.28$ , delay time, 6 ns; and  $\epsilon = 10^{-11}$ . Laser intensity  $E(t)^2$  was found to be amplitude modulated as a result of the interference between the lasing and the frequency-modulated feedback fields. The numerical waveform and the corresponding power spectrum (long-term average) correspond well to the experimental result shown in Figs. 2 and 3. This implies that feedback ratio  $m^2$  in the experiment without the attenuator is estimated to be  $-100$  dB. Some distortion in vibration amplitude [Fig. 4(c)] and broadening of the spectrum of the sidebands [Fig. 4(d)] resulted from spontaneous emission noise in such a weak feedback regime. We obtained a pure sinusoidal vibration waveform by omitting the spontaneous emission term in Eq. (2). In the case of Fig. 3(b) the feedback ratio, which was sufficient for practical measurement, was found to be as small as  $-112$  dB. It should be noted that the frequency modulation index is determined only by feedback ratio  $m^2$  and is independent of the laser output intensity.

Finally, we carried real-time vibration measurements by connecting the photoreceiver output to a frequency demodulation circuit that employed superheterodyne detection with 20-kHz bandwidth at the

intermediate frequency of 10.7 MHz. Demodulated vibration waveforms and their power spectra are shown in Fig. 5 for different modulation frequencies, where vibration amplitudes calibrated based on the results shown in Fig. 3 are also given. Detailed vibration waveforms that show some irregularity and distortions in speaker vibrations, exhibiting higher harmonics, are clearly identified on a nanometer scale.

In summary, an ultrahigh-sensitivity real-time nanometer-vibration measurement of a vibrating target was successfully demonstrated by a self-aligned self-mixing laser Doppler vibrometry technique that used a laser-diode-pumped microchip solid-state laser. Experimental signal characteristics were well reproduced by numerical simulations. The measurement at a  $< -110$ -dB feedback ratio obtained by the present technique may enable us to perform *in situ* analyses of, e.g., moving or vibrating targets embedded in optically diffusive media, tissue biomonitors, cooled atoms, and earthquakes. The almost unheard sound of music from the speaker below a 20-dB sound pressure level was clearly reproduced by the present optical microphony.

K. Otsuka is indebted to F. Stoeckel, E. Lacot, and R. Day of the Université de J. Fourier at Grenoble for discussions. T.-S. Lim was supported by National Science Council, Taiwan, under project NSC90-2112-M-006-018. K. Otsuka's e-mail address is [otsuka@keyaki.cc.u-tokai.ac.jp](mailto:otsuka@keyaki.cc.u-tokai.ac.jp).

## References

1. K. Otsuka, *IEEE J. Quantum Electron.* **QE-15**, 655 (1979).
2. K. Otsuka, *Jpn. J. Appl. Phys.* **31**, L1546 (1992).
3. R. Kawai, Y. Asakawa, and K. Otsuka, *IEEE J. Photon. Technol. Lett.* **11**, 706 (1999).
4. K. Otsuka, R. Kawai, Y. Asakawa, and T. Fukazawa, *Opt. Lett.* **24**, 1862 (1999).
5. E. Lacot, R. Day, and F. Stoeckel, *Opt. Lett.* **24**, 744 (1999).
6. T. Sekine, K. Shimizu, and K. Otsuka, *Proc. SPIE* **4630**, 41 (2002).
7. H. Toda, M. Haruna, and N. Nishihara, *Electron. Lett.* **22**, 982 (1986).
8. H. Toda, M. Haruna, and N. Nishihara, *IEEE J. Lightwave Technol.* **LT-5**, 901 (1987).
9. P. G. Suchocki, J. P. Waters, and M. R. Fernald, *IEEE J. Photon. Technol. Lett.* **2**, 81 (1990).
10. F. F. M. de Mul, L. Scalise, A. L. Petoukhova, M. van Herwijnen, P. Moes, and W. Steenbergen, *Appl. Opt.* **41**, 658 (2002).
11. P. J. de Groot and G. M. Gallatin, *Opt. Lett.* **14**, 165 (1989).
12. M. H. Koelink, F. F. M. de Mul, A. L. Weijers, J. Greve, R. Graaff, A. C. M. Dassel, and J. G. Aarnoudse, *Appl. Opt.* **33**, 5628 (1994).
13. L. Scalise, W. Steenbergen, and F. de Mul, *Appl. Opt.* **25**, 4608 (2001).
14. D. Gabor, *J. IEEE (London)* **93**, 429 (1946).
15. K. Otsuka, J.-Y. Ko, and T. Kubota, *Opt. Lett.* **26**, 638 (2001).
16. J.-Y. Ko, K. Otsuka, and T. Kubota, *Phys. Rev. Lett.* **86**, 4025 (2001).